The SOI DAWN process for three-dimensional silicon micromachining and its applications

Huai-Yuan Chu [a], Chia-Min Lin [b], Weileun Fang [a,b,*]

[a] *Department of Power Mechanical Engineering, National Tsing Hua University, Hsinchu 30013, Taiwan*
[b] *Institute of NanoEngineering and MicroSystems, National Tsing Hua University, Hsinchu 30013, Taiwan*

ABSTRACT

A DRIE assisted wet anisotropic bulk micromachining (DAWN) process is demonstrated to fabricate various three-dimensional MEMS devices on a silicon-on-insulator (SOI) wafer. This SOI DAWN process can realize thin film structures, reinforced (thin film) structures, and thick structures with totally different mechanical characteristics. Various passive and active mechanical components, including flexible springs, rigid structures, and actuators, have been fabricated using the SOI DAWN process and have been further integrated to create MEMS devices which are flexible as well as movable in both in-plane and out-of-plane directions. This SOI DAWN process has been successfully applied to produce various multi-DOF devices made of single crystal silicon (SCS).

© 2008 Elsevier B.V. All rights reserved.

1. Introduction

Micromachining on a silicon-on-insulator (SOI) wafer is regarded as a promising fabrication process. SOI wafers consist of a silicon device layer, separated with a silicon handling substrate by an insulator (buried SiO_2 layer). In general, this process employs the BOSCH deep reactive ion etching (DRIE) process to define the silicon device layer, and then the structure is released by removing the buried SiO_2 layer [1,2]. The etching process of BOSCH DRIE is crystal plane orientation independent and the removal of the buried SiO_2 layer is an isotropic etching process. Hence, various suspended micromachined structures made of single crystal silicon (SCS) are available on SOI. On the other hand, the convex corner undercut effect [3,4] and the characteristics of crystal planes of SCS are not employed in the SOI process. Thus, the micromachined structures available on SOI wafers are limited.

In general, a complete MEMS mechanism consists of active components such as actuators, and passive components such as springs, hinges, linkages, plates, etc. Various MEMS devices are fabricated by using the combination of these passive and active micromachined components. For instance, the scanning mirror [5] is a typical 1-DOF (degree-of-freedom) MEMS device; the position stage [6] is a 2-DOF device; and the three-axis accelerometer [7] is a 3-DOF

device. According to the superior mechanical properties of SCS [8] and the relatively simple fabrication process, many moveable MEMS devices have been implemented onto a SOI wafer. The thickness of SOI MEMS devices (in the out-of-plane direction) has been determined by the thickness of device silicon layer. The bulk and stiff structures such as the mirror plate are realized in this manner; meanwhile the spring also becomes stiff in the out-of-plane direction. Moreover, the structures flexible in the in-plane direction are frequently been implemented on SOI wafer [9,10]. However, it is not straightforward to fabricate SOI MEMS devices flexible in the out-of-plane direction [11].

This study intends to further extend and elaborate the work in [12,13] by using the DRIE assisted wet anisotropic bulk micromachining on SOI wafer (SOI DAWN) process to fabricate three-dimensional MEMS devices with stiffness ranging from 0.1 to 10^4 N/m and a variety of actuators onto a SOI wafer. This process applies the concepts of convex corner compensation and non-(1 1 1) sidewall protection in [14] on the silicon device layer of the SOI wafer. This process integrates both wet anisotropic etching and DRIE. The thick suspended structure formed by the silicon device layer is available after the buried SiO_2 layer is removed. To demonstrate the capability of the SOI DAWN process, various active and passive components have been fabricated and integrated, and multi-DOF devices made of SCS have been produced [15].

2. Concept and fabrication processes

The goal of the SOI DAWN process is to fabricate and integrate various thin film and bulk structures onto a SOI wafer. The

* Corresponding author at: Power Mechanical Engineering Department, National Tsing Hua University, Hsinchu 30013, Taiwan. Tel.: +886 3 5742923; fax: +886 3 5739372.
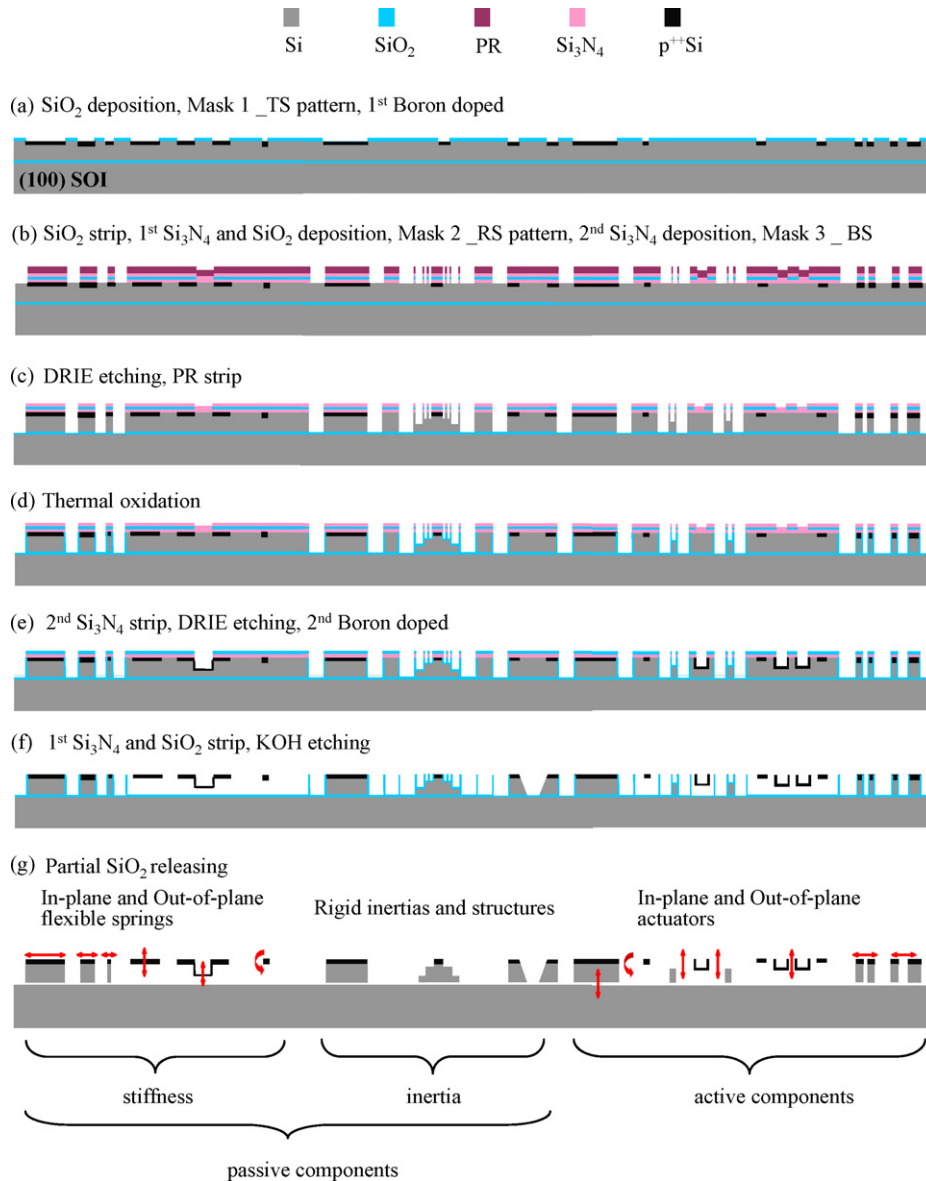*E-mail address:* fang@pme.nthu.edu.tw (W. Fang).

Fig. 1. Flow chart of the SOI DAWN process.

sequence of this three-photo masks fabrication process is illustrated in Fig. 1, which employed the low-resistance (1 0 0) SOI wafer as the substrate. As illustrated in Fig. 1a, the SiO_2 was thermally grown, and then patterned using the 1st photo mask to define the area of boron doping. The SiO_2 layer was removed by diffusion after boron doping. As depicted in Fig. 1b, the Si_3N_4 and SiO_2 films were deposited and then patterned using the second photo mask. After that, the second Si_3N_4 film was deposited and then patterned using the third photo mask. The Si_3N_4 and SiO_2 films in Fig. 1b acted as the etching masks. DRIE was then used to etch through the Si device layer of the SOI wafer, as shown in Fig. 1c. According to the etching lag characteristic of DRIE, various etching depths were realized by tuning the openings of the masks. As illustrated in Fig. 1d, thermal SiO_2 protected the sidewalls of the Si after DRIE. Silicon nitride acted as the mask for the selective thermal oxidation. As shown in Fig. 1e, after removing the second Si_3N_4 film, the second DRIE together with the heavily doped boron was used to tune a cross section of thin film structures. In this step, the SiO_2 film also acted as the mask for the second selective boron diffusion. After the wet anisotropic silicon etching in Fig. 1f, the thin film and reinforced thin film structures (referred to as "reinforced structures" hereafter) were released from the device layer using the convex corner undercut effect. During the wet anisotropic etching process, the non-{1 1 1} crystal planes of the bulk structure were protected by a SiO_2 protection film. The thin structure and the reinforced structure were prevented from etching due to the boron etch-stop effect. As shown in Fig. 1g, the bulk structures were suspended after removing the buried SiO_2 layer underneath; meanwhile, the SiO_2 protection film indicated in Fig. 1f was also etched away.

As indicated in Fig. 1g, the available structures have been characterized as passive and active mechanical components. The passive components consist of flexible springs and rigid inertias; and the active components include various actuators. The black region indicates thin film and U-shape reinforced structures [16]. The thickness of these structures ranges from submicron to several microns, and is determined by the heavily boron doped process. The thin film structure is flexible in the out-of-plane direction allowing it to act as the linear as well as the torsional springs in the out-of-plane direction. The cross section of the thin film structure can
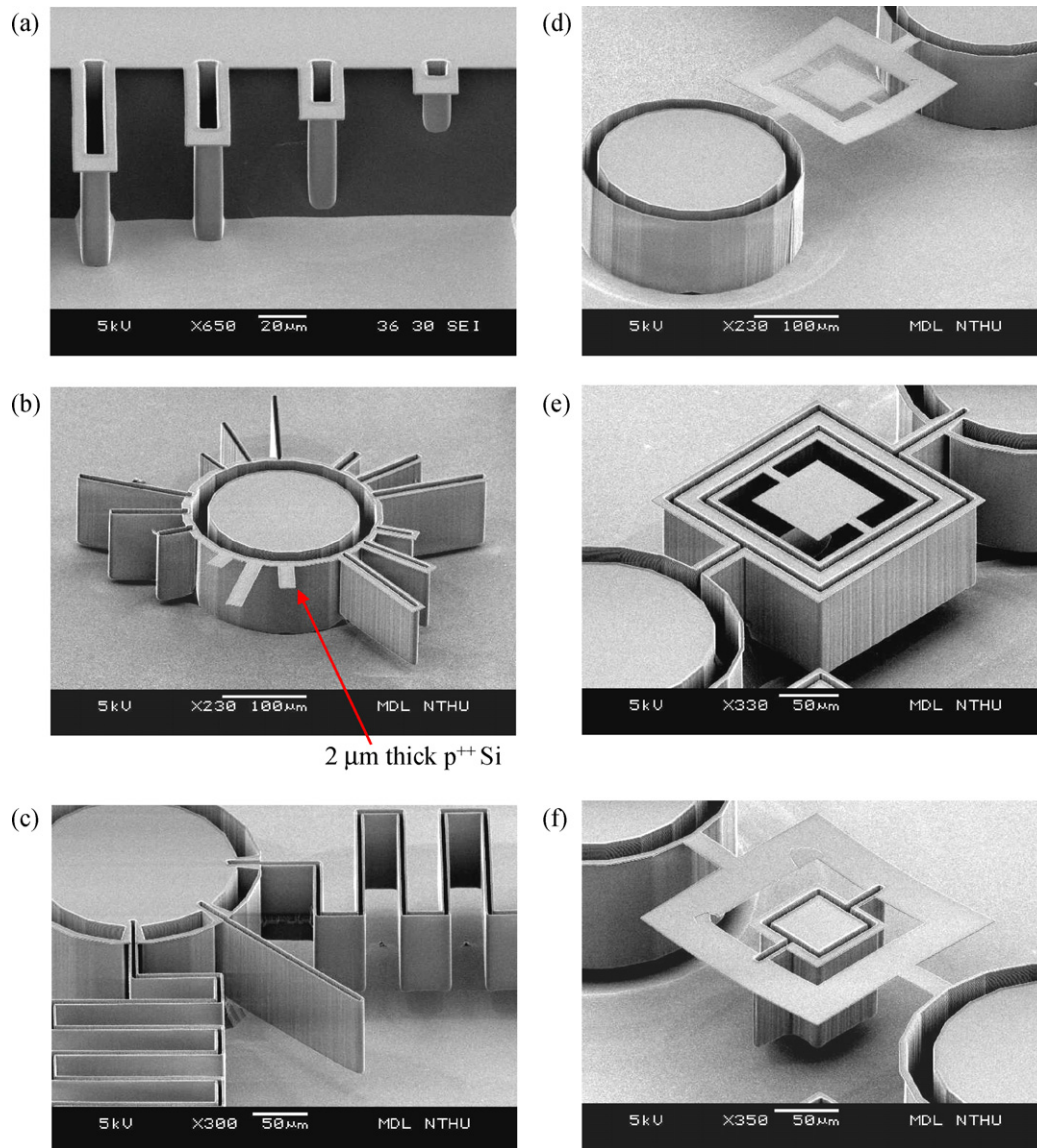
Fig. 2. SEM micrographs showing (a) reinforced thin film cantilevers with different stiffness; (b) thin film and reinforced thin film cantilevers fixed to a mesa; (c) a folded spring formed by the reinforced thin film; (d) a thin film gimbaled structure supported by two circular mesas; (e) a reinforced supporting frame of a thin film gimbaled structure; (f) the reinforced inner stage of a thin film gimbaled structure.

be modified in Fig. 1e. This approach can further be employed to modify the stiffness of the U-shape reinforced structure indicated in Fig. 1g. According to the analysis in [17], the bending stiffness of a 2 μm thick U-shape reinforced structure increases from 10- to 145-fold as the DRIE etching depth in Fig. 1e increases from 1 to 10 μm. As indicated in Fig. 1g, some of the reinforced structure has a higher stiffness-to-mass ratio and can be employed to act as a rigid component, such as a proof mass, mirror plate, position stage, etc. The stiffness-to-mass ratio of the reinforced structure makes it ideal for various applications; for example, a reinforced mirror has a higher scanning frequency [5,18]. The gray region shows the bulk structures with thickness determined by the device layer. The thick structure of smaller width is flexible in the in-plane direction, and acts as an in-plane linear spring. The width of the bulk structure and the spring constant are tuned by using the photolithography process in Fig. 1a and b. A bulk structure of larger width as indicated in Fig. 1g will act as a rigid inertia component. Since the aforementioned thin film and bulk structures can be fabricated and integrated using the SOI DAWN process, fabrication

of 3D MEMS structures with a wider range of mechanical characteristics becomes possible, significantly improving the variety and performance of the micromachined devices.

3. Fabrication results and basic components

To demonstrate the feasibility of this study, various micromachined structures have been designed, fabricated, and integrated using the process in Fig. 1. This section will introduce the fabrication results, and then show various basic passive and active components such as rigid inertia, flexible springs, and actuators realized using the SOI DAWN process.

3.1. Suspended thin film, reinforced, and bulk structures

Fig. 2 shows various thin film structures and reinforced structures. The SEM photos in Fig. 2b show suspended thin film and reinforced cantilevers, made of 2 μm thick p^{++} Si, fixed to a thick circular mesa. The rib defined by the second DRIE in Fig. 1e is 100 μm
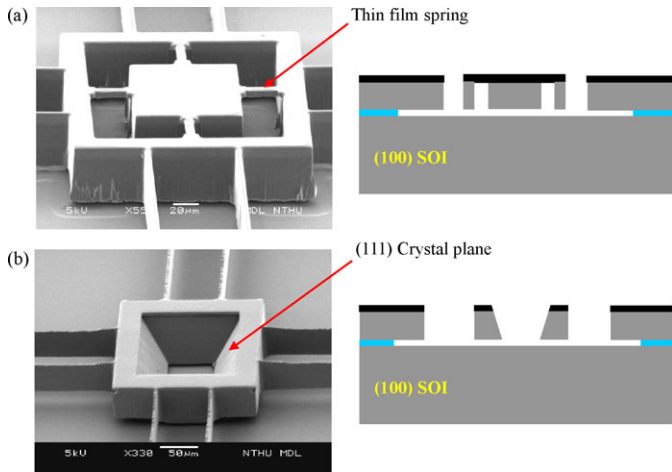
Fig. 3. Typical rigid structures realized by the SOI DAWN process: (a) rigid inertia and frame integrated with suspended thin film springs; (b) rigid inertia with a cavity formed by (1 1 1) crystal planes.

Fig. 4. Typical springs available by the SOI DAWN process: (a) in-plane bending springs; (b) out-of plane torsional spring; (c) out-of plane bending spring.

in depth; and the bending stiffness (in the out-of-plane direction) of the reinforced cantilever increased nearly 3000-fold, as predicted by the analysis in [17]. Fig. 2c shows a folded spring formed by the reinforced thin film. The hollow reinforced structure is clearly observed. According to finite element analysis, the out-of-plane bending stiffness of the reinforced folded spring increased by three orders of magnitude as the DRIE depth in Fig. 1e exceeds 100 μm.

The position of the reinforced structure can be defined by the photolithography in Fig. 1a and b. Thin film structure can be reinforced only at some particular portions. As a result, both flexible and stiff structures were fabricated and integrated using the same film. Fig. 2d–f shows typical examples of the combination of thin film and reinforced structures. Fig. 2d shows a thin film gimbaled structure supported by two circular mesas. The gimbaled structure mainly consisted of two torsional springs, one supporting frame, and one inner plate. By comparison, the supporting frame of the gimbaled structure in Fig. 2e was replaced by a reinforced structure; however, the inner plate and its torsional spring remained thin film structures. In this case, the supporting frame was regarded as a rigid component. According to finite element analysis, the stiffness of this reinforced frame increased 18,000-fold. In Fig. 2f, the inner plate and its torsional spring were replaced by a reinforced structure; however, the supporting frame remained a thin film structure. The stiffness of the reinforced plate was increased 4300-fold as predicted by finite element analysis.

It is well known that suspended bulk rigid structures can be directly implemented using the device silicon layer of a SOI wafer. A typical example shown in Fig. 3a is the 60 μm thick rigid frame and rigid inertia. SOI DAWN can further integrate these bulk rigid structures with the suspended thin film springs, as indicated in Fig. 3a. SOI DAWN also employed silicon anisotropic etching to fabricate a cavity with (1 1 1) crystal planes on the rigid inertia, as shown in Fig. 3b.

3.2. In-plane and out-of-plane springs

The suspended thin films, reinforced, and bulk structures fabricated by SOI DAWN offer springs with totally different mechanical characteristics, as demonstrated in Fig. 4. As shown in Fig. 4a, a rigid mass was supported by eight springs made of a 60 μm thick device layer. These bulk structures acted as the in-plane linear spring. The thickness of the in-plane spring offered a high stiffness in the out-of-plane direction preventing unwanted out-of-plane motion. The
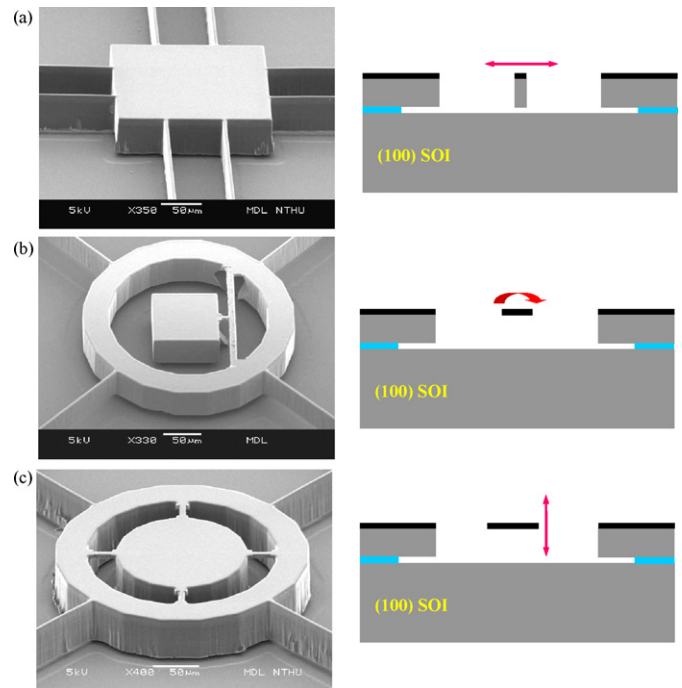
planar shape and dimensions of these in-plane springs were determined by photolithography. Thus, the in-plane spring stiffness was easily adjusted by the fabrication process. Fig. 4b demonstrates a thin torsional spring, which allowed the rigid block to move angularly in the out-of-plane direction. The circular rigid mass in Fig. 4c was supported by four 2 μm thick p^{++} Si structures. These thin film structures acted as the linear out-of-plane spring. The rigid mass moved in the out-of-plane direction when these thin structures were bent. In addition, the thin linear and torsional springs in Fig. 4b and c were connected to a bulk rigid frame, which was supported by four bulk in-plane springs. In short, the SOI DAWN successfully demonstrated its capability of integrating various bulk and thin films to increase the degrees of freedom of micromachined components.

3.3. In-plane actuators

Many in-plane these high-aspect-ratio-MEMS (HARM) actuators fabricated using the device silicon layer of a SOI wafer have already been reported in [4]. The SOI DAWN process was able to implement these in-plane HARM actuators using a device silicon layer, and three typical results are shown in Fig. 5a–c. Fig. 5a shows a comb-drive electrostatic actuator array; and Fig. 5b is a parallel plate gap-closing electrostatic actuator array. A hot–cold beam electrothermal actuator array is shown in Fig. 5c. Since these actuators consisted of 60 μm thick HARM structures, the coupling of unwanted out-of-plane motion was prevented. The thin film in-plane actuators were achieved using the SOI DAWN process. Fig. 5d shows a hot–cold beam electrothermal actuator made of 1 μm thick p^{++} silicon.

3.4. Out-of-plane actuators

The presented SOI DAWN process has already realized various out-of-plane actuators, as demonstrated in Fig. 6. Fig. 6a shows a vertical-comb electrostatic actuator. The partially trimmed silicon
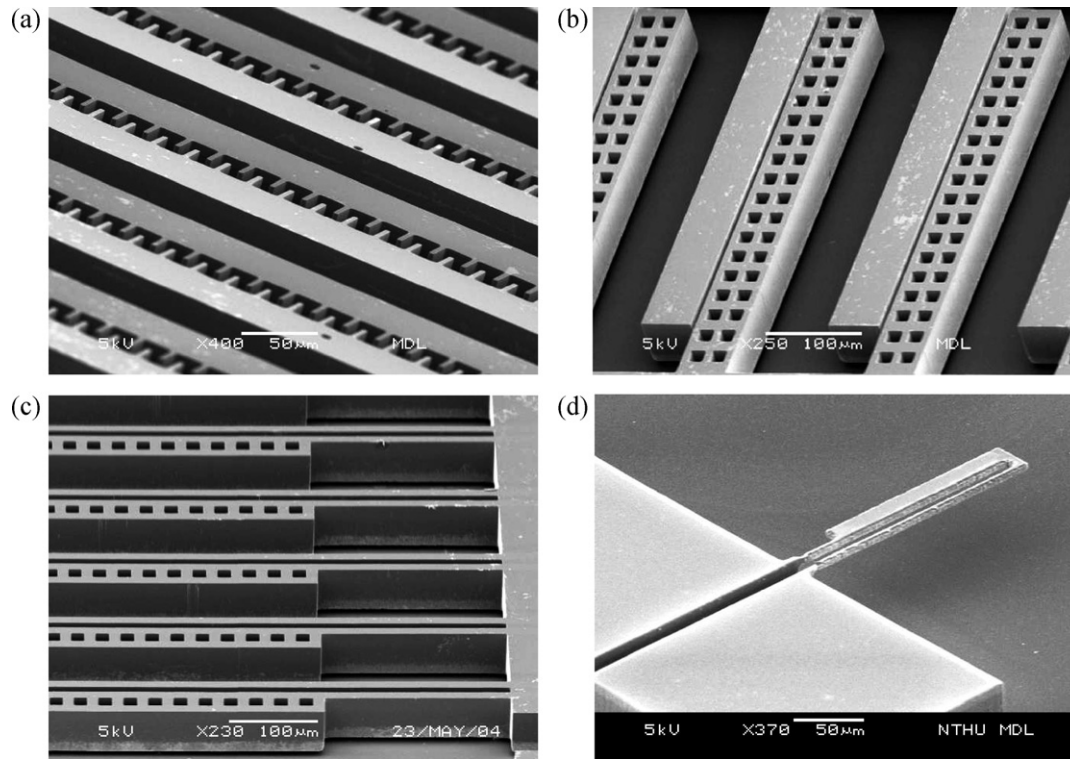
Fig. 5. Typical in-plane actuators fabricated by the SOI DAWN process: (a) HARM comb drive actuator; (b) HARM gap-closing actuator; (c) HARM hot–cold-beam thermal actuator; (d) thin film thermal actuator.

device layer was anchored to the substrate, and acted as stationary comb electrodes. The p^{++} Si reinforced structure acted as the moving electrodes. Fig. 6b demonstrates a gap-closing electrostatic actuator. The handling wafer in Fig. 6b acted as the stationary electrode, whereas the rigid mass made of a bulk device layer acted
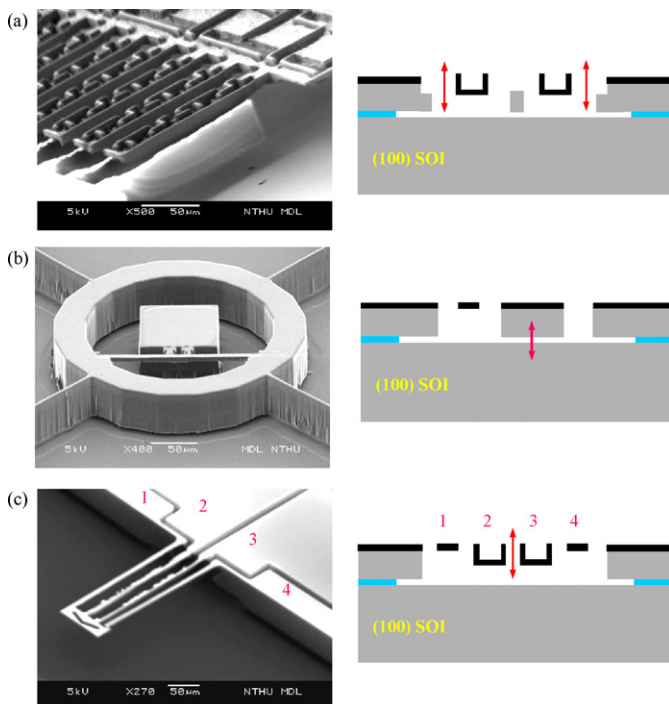

Fig. 6. Typical out-of-plane actuators available by the SOI DAWN process (a) vertical comb actuator; (b) gap-closing actuator; (c) bi-directional electrothermal actuator.

as the moving electrode. In addition, this study utilized the concept reported in [19] to fabricate the bi-directional out-of-plane electrothermal actuators using the p^{++} Si film. As depicted by the illustration in Fig. 6c, the thermal actuator consisted of four beams located at different depths. The two outer beams expanded and caused the actuator to move downward when the current flowed from pad 1 to pad 4. The two inner beams expanded and led to the moving upward of the actuator when the current flowed from pad 2 to pad 3.

4. Components integration and applications

The micromachined structures and components presented in Figs. 2–6 were all fabricated using the SOI DAWN fabrication platform. Further establishing the capability of the SOI DAWN process, the multi-DOF MEMS devices were demonstrated by monolithically integrating the components in Figs. 2–6.

4.1. 1-DOF MEMS device

Two typical examples of 1-DOF devices are the moving stages shown in Figs. 7 and 8. The moving stage in Fig. 7 consists of two thin film torsional springs, a reinforced plate, and vertical comb actuators shown in Fig. 6a. The moving stage has angular displacement when driven by the vertical comb actuators. The measurement results in Fig. 7b show the variation of the angular displacement and the driving voltage. The angular displacement is near 1.3° with a driving voltage of 50 V. The moving stage in Fig. 8 consists of a bulk rigid block, and the thin film thermal actuator shown in Fig. 6c. The moving stage has linear displacement when driven by the thermal actuator. The measurement results in Fig. 8b show the variation of the linear displacement and the driving voltage. The out-of-plane displacement was observed to be 3.25 μm for a driving voltage of 8 V.
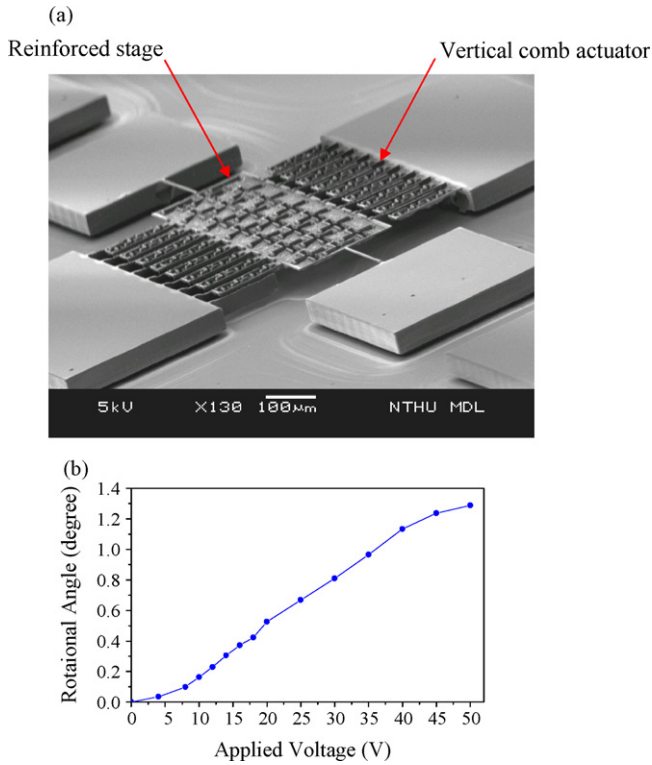
Fig. 7. A 1-DOF torsional moving stage: (a) the moving stage consists of two thin film torsional springs, a reinforced plate, and vertical comb actuators; (b) measured angular displacements versus driving voltages of the stage.

Other examples are available in Fig. 9. Fig. 9a shows a linear moving stage consisting of a bulk platform, bulk linear comb actuators, and reinforced thin film suspension. The comb electrodes were made of a device silicon layer, so as to increase the electrostatic driving force. The reinforced folded spring was exploited to significantly reduce the in-plane stiffness and to reduce the driv-
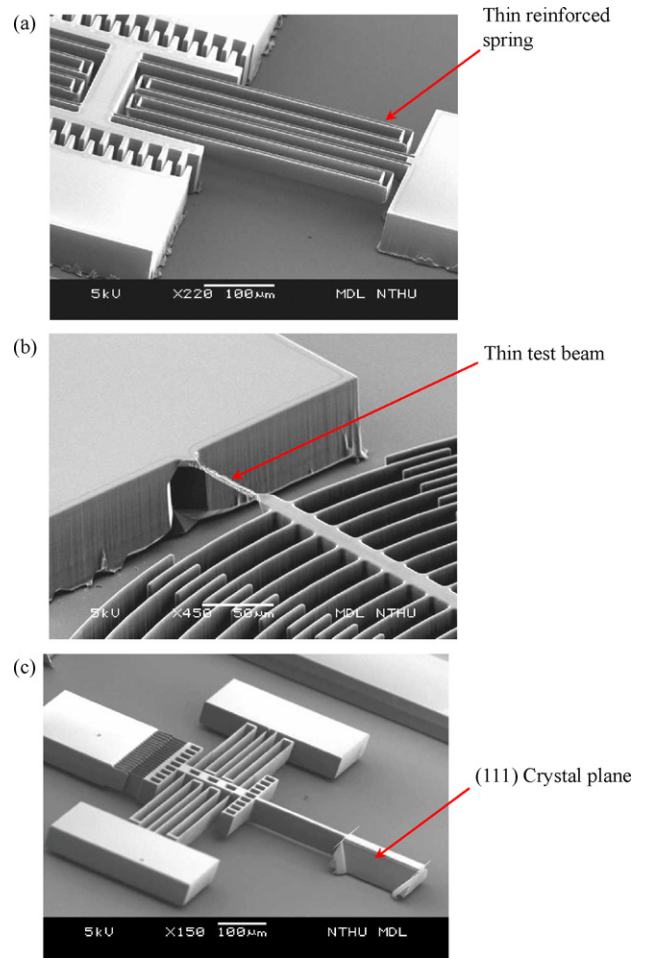

Fig. 8. A 1-DOF linear moving stage: (a) the moving stage consists of a bulk rigid block and a thin film electrothermal actuator; (b) measured linear displacements versus driving voltages of the stage.

Fig. 9. Other 1-DOF MEMS devices available by the SOI DAWN process: (a) a bulk linear moving stage supported by reinforced folded springs; (b) a thin film specimen monolithically connected to a bulk Si comb actuator for bending test; (c) a linear position stage with sidewalls of (1 1 1) crystal plane for optical applications.

ing voltage, while its out-of-plane stiffness remained large enough to support the actuator. Fig. 9b shows an on-chip test stand for thin film material testing. The test stand consists of bulk angular comb drive actuators supported by bulk folded suspensions. A very thin test beam with a thickness of less than 2 μm was monolithically connected to this actuator after the fabrication process. The comb actuator was designed to conduct a bending test on the thin film eliminating the need for assembly and alignment of the actuator and test specimen. Fig. 9c shows a linear position stage for optical applications. The position of the block with sidewalls of (1 1 1) crystal plane was precisely tuned by the linear moving platform.
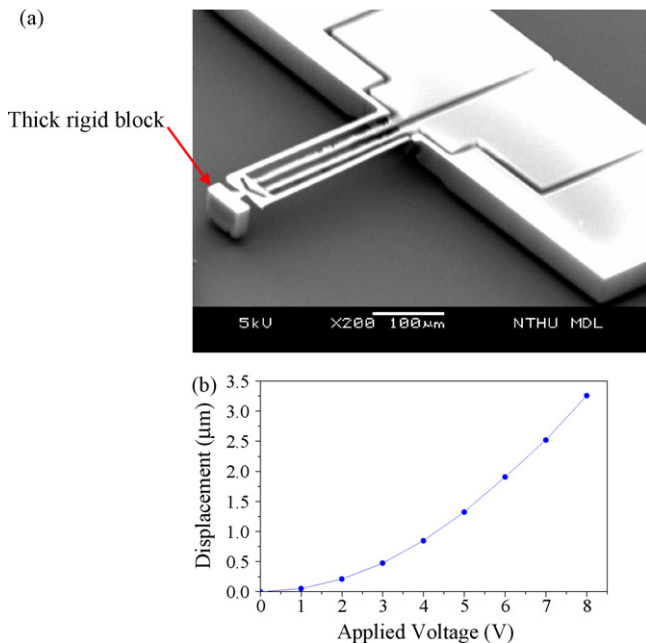
4.2. 2-DOF MEMS devices

Figs. 10 and 11 demonstrate a 2-DOF position stage and a 2-DOF probe, respectively. The 2-DOF position stage in Fig. 10a can move linearly and angularly in the out-of-plane direction. This rigid bulk stage was supported and driven by the out-of-plane electrothermal actuators shown in Fig. 6c. The stage experienced a linear out-of-plane motion when both actuators moved in the same direction. However, the stage experienced an angular out-of-plane motion when these two actuators moved in the opposite direction. The measurement results in Fig. 10b show the variation of the linear and angular displacements with the driving voltage, respectively.
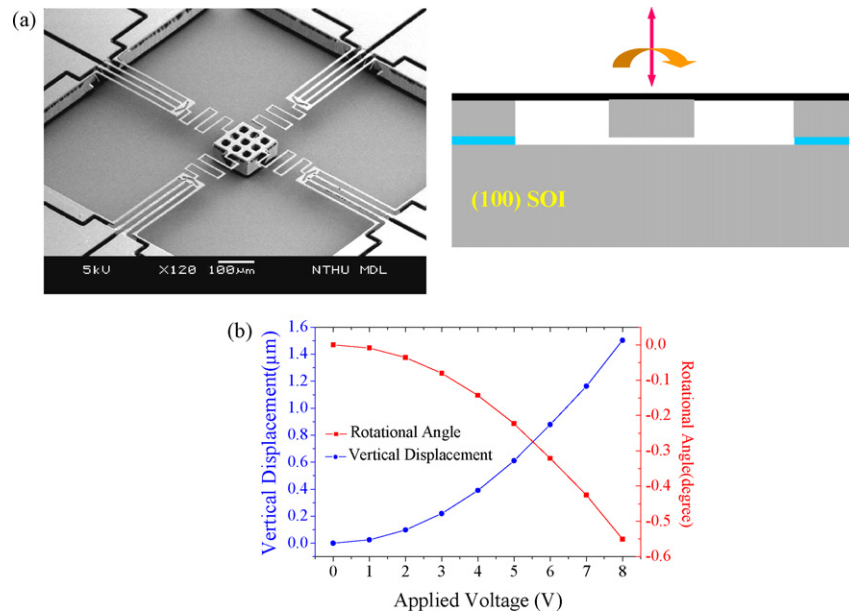
Fig. 10. A 2-DOF position stage: (a) the SEM photo of the stage; (b) measured out-of-plane linear displacements (circular dots) and angular displacements (square dots) versus driving voltages of the 2-DOF position stage.

Fig. 11a shows a bulk probe suspended by the thin film hot–cold beam actuator array. This 2-DOF probe made of a bulk device layer can move linearly in both in-plane and out-of-plane directions. As discussed in Fig. 5d, these hot–cold beam thermal actuators were used to drive the probe linearly in the in-plane direction. In addition, these thin actuators also acted as the out-of-plane bending

springs. The out-of-plane motion of the probe was driven by the gap-closing electrodes presented in Fig. 6b. The probe and handling wafers acted as the moving and stationary electrodes, respectively. The measurement results in Fig. 11b, respectively, show the variation of the in-plane and out-of-plane linear displacements with the driving voltage.
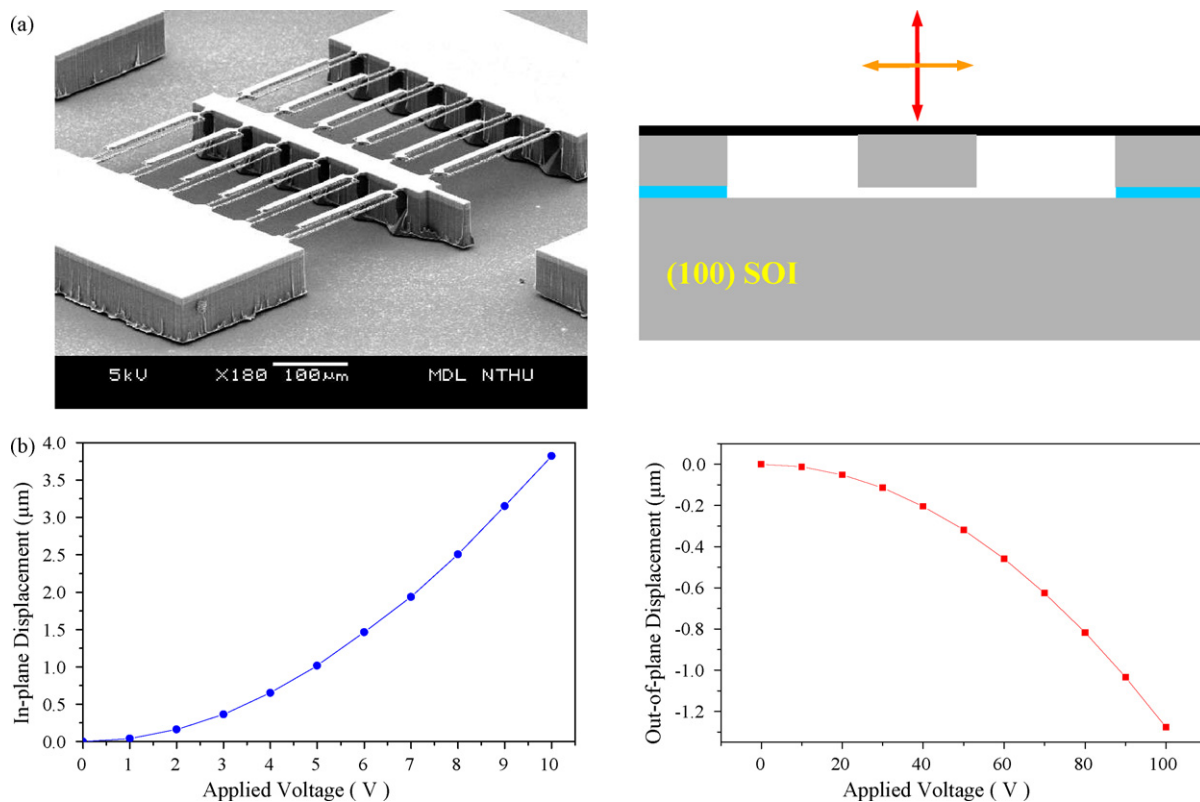

Fig. 11. A 2-DOF bulk probe: (a) SEM photo of the probe; (b) measured in-plane displacements (left) and out-of-plane displacements (right) versus driving voltages of the 2-DOF bulk probe.
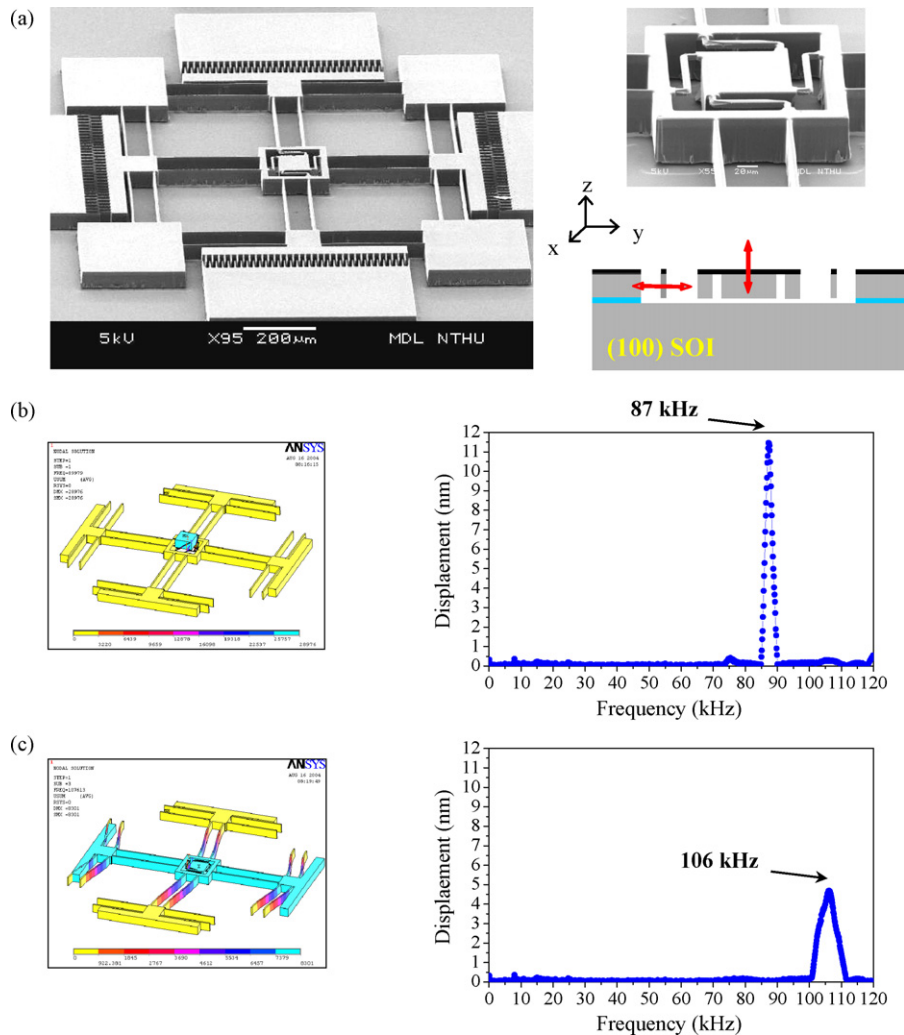
Fig. 12. A 3-DOF position stage which can move linearly in both in-plane and out-of-plane directions: (a) SEM photos of the stage; (b) measured frequency response and its simulated mode shape of the out-of-plane mode driven by the comb-drive actuator; (c) the measured frequency response and its simulated mode shape of the in-plane mode driven by the gap-closing actuator.

4.3. 3-DOF MEMS device

Fig. 12a shows a 3-DOF-position stage, which is designed to move linearly in two in-plane and one out-of-plane directions. The linear comb-drive actuators depicted in Fig. 5a drove the in-plane motion, and the gap-closing actuator presented in Fig. 6b drove the out-of-plane motion. The close-up SEM photo in Fig. 12a indicates that the bulk rigid stage is connected to a rigid frame by four serpentine thin film springs. In addition, the rigid frame is supported by four bulk dual-beam springs. The bulk dual-beam spring was 60 μm thick by 6 μm wide and the thin serpentine spring was 2 μm thick by 12 μm wide. The bulk dual-beam springs together with the comb-drive actuators only allow the stage to move in either the x-axis or y-axis (in-plane) direction [5]. The serpentine thin spring together with the gap-closing electrodes allow the stage to only move in the z-axis (out-of-plane) direction. The measured frequency responses and the mode shapes predicted by ANSYS are shown in Fig. 12b and c. The FEM simulation results show that the motions of the movable platform in the x-, y-, and z-axes can be controlled independently. The out-of-plane mode measured by a commercial Laser Doppler Vibrometer (LDV) was 87 kHz. Since the dynamic characteristics of the platform were designed to be symmetrical in the x-and y-axes, the in-plane modes measured by LDV were 106 kHz.

5. Conclusions

This study has demonstrated a DRIE assisted wet anisotropic bulk micromachining process to fabricate various three-dimensional MEMS devices on a SOI wafer. In addition to micromachined structures realizable by wet anisotropic etching and DRIE, this process can also fabricate micromachined structures using the device layer of a SOI wafer. Thus, the presented SOI DAWN process can realize and integrate thin film structures, reinforced structures, and bulk HARM structures. Moreover, various passive and active mechanical components have also been developed and reported, for instance, the in-plane and out-of-plane springs and actuators, and rigid inertia. SOI DAWN can be used to integrate these components to create various MEMS devices. In this study, MEMS devices with 1–3 DOF have been demonstrated. Since SOI DAWN only needs three masks, and no critical alignment and bonding process is required, it has the potential to become a very useful and promising fabrication platform for MEMS.

Acknowledgements

References

[1] T.D. Kudrle, H.P. Neves, D.C. Rodger, N.C. MacDonald, A microactuated millimeter wave phase shifter, in: Transducers'99, Sendai, Japan, June, 1999, pp. 1276–1279.

[2] M.E. McNie, D.O. King, M.C.L. Ward, Micromachining in SOI, in: Recent Advances in Micromachining Techniques IEE Colloquium, 20 November, 1997, pp. 5/1–5/4.

[3] H. Jansen, M. de Boer, M. Elwenspoek, Black silicon method VI: High aspect ratio trench etching for MEMS applications, in: IEEE MEMS'96, San Diego, CA, February, 1996, pp. 250–257.

[4] M. de Boer, H. Jansen, M. Elwensspoek, The black silicon method V: A study of the fabricating of movable structures for micro electromechanical systems, in: Tansducers'95, Stockholm, Sweden, June, 1995, pp. 565–568.

[5] H.-Y. Lin, W. Fang, A reinforced micro-torsional-mirror driven by electrostatic torque generators, Sens. Actuators A 105 (2003) 1–9.

[6] V.P. Jaecklin, C. Linder, N.F. de Rooij, J.M. Moret, R. Bischof, F. Rudolf, Novel polysilicon comb actuators for xy-stages, in: IEEE MEMS'92, Las Vegas, NV, January, 2002, pp. 147–149.

[7] K.I. Lee, H. Takao, K. Sawada, M. Ishida, Low temperature dependence three-axis accelerometer for high temperature environments with temperature control of SOI piezoresistors, Sens. Actuators A 104 (2003) 53–60.

[8] K.E. Petersen, Silicon as a mechanical material, Proc. IEEE 70 (1982) 420–457.

[9] A. Sharma, M.F. Zaman, B.V. Amini, F. Ayazi, A high Q in-plane silicon-on-insulator tuning-fork gyroscope, in: IEEE Sensors'04, Vienna, Austria, October, 2004, pp. 467–470.

[10] Z.F. Wang, W. Caob, X.C. Shan, J.F. Xu, S.P. Lim, W. Noell, N.F. de Rooij, Development of 1 × 4 MEMS-based optical switch, Sens. Actuators A 114 (2004) 80–87.

[11] V. Milanovic, M. Last, K.S.J. Pister, Laterally actuated torsional micromirrors for large static deflection, IEEE Photon. Technol. Lett. 15 (2003) 245–247.

[12] H.-Y. Chu, W. Fang, Fabrication of 3D microstructures and microactuators on (1 0 0) SOI wafer using the DAWN process, in: IEEE MEMS'04, Maastricht, The Netherlands, January, 2004, pp. 753–756.

[13] H.-Y. Chu, W. Fang, Bulk micromachining fabrication platform using the integration of DRIE and wet anisotropic etching, Microsyst. Technol. 11 (2005) 141–150.

[14] H.-Y. Chu, W. Fang, A vertical convex corner compensation and non-{1 1 1} crystal planes protection for wet anisotropic bulk micromachining process, J. Micromech. Microeng. 14 (2004) 806–813.

[15] H.-Y. Chu, W. Fang, A novel vertical convex corner compensation for wet anisotropic bulk micromachining, in: IEEE MEMS'04, Maastricht, The Netherlands, January, 2004, pp. 253–256.

[16] H.-Y. Lin, W. Fang, The rib-reinforced micromachined beam and its application, J. Micromech. Microeng. 10 (2000) 93–99.

[17] F.P. Beer, E.R. Johnston Jr., Mechanics of Materials, McGraw-Hill, New York, NY, 1992.

[18] M. Wu, W. Fang, Design and fabrication of MEMS devices using the integration of MUMPs, trench-refilled molding, DRIE and bulk silicon etching processes, J. Micromech. Microeng. 15 (2005) 535–542.

[19] W.-C. Chen, C.-C. Chu, J. Hsieh, W. Fang, A novel single-layer bi-directional out-of-plane electrothermal microactuator, Sens. Actuators A 103 (2003) 48–58.

Biographies

Huai-Yuan Chu was born in Taipei, Taiwan 1977. He received his MS and PhD degree in power mechanical engineering department, National Tsing Hua University, Taiwan, in 2002 and 2005, respectively. His research interests include MEMS applications in printing systems, CNT-MEMS and micro bio-system for neural recording. He is currently working at Micromachine Product Division, ADI, as a senior process development engineer.

Chia-Min Lin was born in Hsinchu, Taiwan, in 1982. He received his master degree from the Institute of NanoEngineering and MicroSystems, National Tsing Hua University, Taiwan in 2006. Currently he is studying for PhD degree in the Institute of NanoEngineering and MicroSystems, National Tsing Hua University, Taiwan. His major research interests include polymer MEMS, and CNT-MEMS.

Weileun Fang was born in Taipei, Taiwan, in 1962. He received his PhD degree from Carnegie Mellon University in 1995. His doctoral research focused on determining of the mechanical properties of thin films using micromachined structures. In 1995, he worked as a postdoctoral researcher at Synchrotron Radiation Research Center, Taiwan. He joined the Power Mechanical Engineering Department at the National Tsing Hua University (Taiwan) in 1996, where he is now a Professor as well as a faculty of NEMS Institute. He served as the TPC of IEEE MEMS'04 and IEEE MEMS'07, and the regional TPC of Transducers'07. He is now on the Editorial Board of *JMM*. He has established a MEMS testing and characterization lab. His research interests include MEMS with emphasis on microfabrication/packaging technologies, microoptical systems, microactuators, and the characterization of the mechanical properties of thin films.